CHAPTER THREE

Decline in PABPN1 expression level marks skeletal muscle aging

Seyed Yahya Anvar[1,*], Yotam Raz[2], Andrea Venema[1], Merel L.R. van 't Hoff[1], Marius Gheorghe[1], Jelle J. Goeman[3], Barbara van der Sluijs[4], Baziel van Engelen[4], Marc Snoeck[5], John Vissing[6], Silvère M. van der Maarel[1], Peter A.C. 't Hoen[1] and Vered Raz[1,*]

Aging-associated disorders can be accompanied by increased tissue degeneration and may provide insight into key regulators of aging. Oculopharyngeal muscular dystrophy (OPMD) is caused by alanine-expansion mutations in *PABPN1,* and is characterized by progressive skeletal muscle weakness that is manifested after midlife. We compared expression profiles from *Vastus lateralis* of controls and OPMD. Similar to PABPN1 expression, between 40-45 years a transcriptional switch was identified in both OPMD and muscle aging while trends in OPMD were accelerated. Among these genes, we identified a significant and progressive decline in *PABPN1* expression from the fifth decade in aging muscles. In concurrence with the more severe muscle weakness, this decline was accelerated in muscles primarily affected in OPMD. The aging-associated decline of *PABPN1* was not detected in other tissues or in blood from OPMD patients. We show that down-regulation of *PABPN1* induced progressive cell senescence in myoblast cultures. We suggest that a decline in *PABPN1* expression marks muscle aging and reduced levels of the protein causes age-associated muscle degeneration.

1 Center for Human and Clinical Genetics, Leiden University Medical Center, Leiden, the Netherlands. **2** Department of Gerontology and Geriatrics, Leiden University Medical Center, Leiden, the Netherlands. **3** Department of Medical Statistics and Bioinformatics, Leiden University Medical Center, Leiden, the Netherlands. **4** Department of Neurology, Radboud University Nijmegen Medical Center, Nijmegen, the Netherlands. **5** Department of Anaesthesia, Canisius-Wilhelmina Hospital, Nijmegen, the Netherlands. **6** Neuromuscular Research Unit and Department of Neurology, Rigshospitalet Copenhagen, Copenhagen, Denmark.

* To whom correspondence should be addressed at: v.raz@lumc.nl

Manuscript Submitted, 2012

INTRODUCTION

Aging is marked by a progressive decline of cellular activities and its rate differs between tissues (Kirkwood and Austad, 2000). A decrease in skeletal muscle performance, as measured by strength, highly correlates with biological aging. Age-associated muscle weakness in healthy cohorts starts around the fifth decade and linearly progresses with age (Beenakker et al., 2010). A decline in muscle strength is suggested to predict functional disability and mortality in elderly (Liu and Latham, 2011; Ling et al., 2010; Roth et al., 2002). The degenerative loss of muscle function during aging is regulated by numerous genetic and environmental factors. Consequently, the onset and progression of aging-associated decline in muscle performance vary greatly between individuals. Aging is a complex process and the molecular mechanisms that control the onset and progression of muscle aging, as well as key regulators, are not fully understood. The high complexity of aging-associated molecular mechanisms is demonstrated by genome-wide changes in mRNA expression affecting a broad range of biological processes. Genome-wide transcriptional changes can be derived by changes in mRNA stability. Thus, it is expected that regulators of mRNA processing would regulate aging-associated transcriptional changes.

Aging associated changes can sometimes be exacerbated in patients with late onset degenerative disorders (Kirkwood and Austad, 2000). Studies of late onset disorders can thereby expose key regulators of aging that are otherwise difficult to identify. Oculopharyngeal muscular dystrophy (OPMD) is a late onset autosomal dominant muscle disorder. OPMD is characterized by progressive ptosis, dysphagia, and proximal limb muscle weakness that typically appear from the fifth decade (Brais et al., 1995; Taylor, 1915; van der Sluijs et al., 2003). OPMD is caused by a trinucleotide repeat expansion mutation in the gene encoding for *Poly(A) Binding Protein Nuclear 1* (*PABPN1*) causing a poly-alanine expansion in the N-terminus of PABPN1 (expPABPN1) (Brais et al., 1998). PABPN1 binds to mRNA and regulates poly(A) elongation (Benoit et al., 2005). The length of poly(A) depends on PABPN1 concentration (Kuhn et al., 2009), and knockdown of PABPN1 causes shortening of poly(A) tail mRNA (Apponi et al., 2010). PABPN1 knockdown in mouse myotubes leads to myogenic defects and reduced cell fusion (Apponi et al., 2010). Reduced cell fusion was also reported in OPMD myoblast cultures (Perie et al., 2006). Overexpression of mutant PABPN1 also leads to muscle cell defects in a mouse model (Davies et al., 2005; Trollet et al., 2010). Mutant PABPN1 is prone to aggregation and accumulates in insoluble nuclear inclusions (Tome and Fardeau, 1980). Although prevention of protein aggregation in animal models with high overexpression of expPABPN1 are effective in delay of muscle weakness (Davies et al., 2005; Chartier et al., 2009; Catoire et al., 2008), aggregation of wild-type PABPN1 were also reported in aging rat neuron cells (Berciano et al., 2004). In contrast to aggregates of expAPBPN1, those of the wild type protein are not disease-associated. In cell models both wild type and expPABPN1 form aggregates, while expPABPN1 is more prone to aggregation (Raz et al., 2011a; Raz et al., 2011b). Differences in aggregation can be, in part, explained in differences in poly-ubiquitination (Raz et al., 2011b). Inhibition of the proteasome enhances the aggregation of expPABPN1 in cell models (Abu-Baker et al., 2003; Raz et al., 2011b). In OPMD the ubiquitin-proteasome system (UPS) is significantly deregulated (Anvar et al., 2011; Raz et al., 2011b). Dysfunctional UPS stimulates the formation of many protein aggregates (Balch et al., 2008; Morimoto, 2008; Sherman and Goldberg, 2001).

It is unclear how a ubiquitously expressed protein, like PABPBN1, predominantly affects only a subset of skeletal muscles and causes symptoms that are not apparent until midlife. We hypothesized that aging contributes to the initiation and progressiveness of muscle weakness in OPMD. We investigated the hypothesis that aging factors contribute to OPMD. We identified signifi-

cant similarities between OPMD-deregulated and aging–regulated expression profiles. In concurrence with muscle symptoms in OPMD, transcriptional changes were accelerated in OPMD compared with normal aging. We show that a decline in PABPN1 expression is highly correlated with age-associated changes in muscle strength in both OPMD and in muscle aging. We show that down regulation of PABPN1 induces cell senescence. Since PABPN1 regulates mRNA stability, we suggest that changes in PABPN1 expression levels in muscle cells would lead to broad transcriptional changes and hence muscle weakness.

RESULTS

Molecular signatures of aging are found in the OPMD mouse model at young age

Symptoms in OPMD do not become apparent until midlife. Therefore, we hypothesised that molecular processes that control muscle aging are involved in OPMD pathogenesis. We investigated whether aging-regulated genes are deregulated in a mouse model for OPMD. In the A17.1 mouse expPABPN1 is overexpressed in muscles leading to muscle weakness (Davies et al., 2005). In this mouse model, muscle atrophy initiates after 12 weeks (Trollet et al., 2010). A17.1-deregulated genes were identified from age-matched wild type controls (Trollet et al., 2010). In a literature-aided association study (LAS), we observed a large subset of A17.1-deregulated genes, in 6 week-old A17.1 mice, that were strongly associated with the term '*Aging*' (**Figure 1A**). Moreover, the fold-change of these genes was remarkably high (**Figure 1A**). This suggests that in this mouse model aging-associated transcriptional changes are induced already at 6 weeks. In an unsupervised meta-analysis, 104 microarray studies, which are related to muscle development and muscle disorders, were compared with that of A17.1. Three major clusters of similar transcriptional changes were identified (**Figure 1B**). The transcriptome of the 6 week-old A17.1 mouse was clustered together with those related to skeletal muscle aging (Welle et al., 2004; Giresi et al., 2005), but not with datasets from other muscular dystrophies or myopathies (**Figure 1B**). These analyses further indicate that transcriptional changes in OPMD are highly associated with those of muscle aging.

Common molecular signatures in muscle aging and OPMD

To investigate genome-wide transcriptional changes in OPMD and during aging in humans, three microarray datasets were generated from *Vastus Lateralis* muscles. For muscle aging a continuous cross sectional dataset was generated from controls aged 17-89. Datasets from OPMD and expPABPN1 carries at pre-symptomatic stage were generated after comparing to age-matching control groups (**Supplementary Table 1**). Major sources of transcriptional variation were assessed using unsupervised principal component analysis (PCA). In the control dataset age-associated variations were identified using the first three principal components, covering 49% of transcriptional variation. Based on the PCA analysis, samples were clustered into two age groups of 17-42 and 43-89 years (**Figure 2A**). This suggests a genome-wide transcriptional switch at the first half of the fifth decade. To verify this, we analysed the expression trends of probes whose expression changed with age (named here as aging-regulated; $P<0.05$). We identified a major switch-point around the age of 42±5 years (**Figure 2A**). An absolute correlation distance measure of k-means clustering revealed that the up-regulated and down-regulated trends of 70% of the age-regulated probes are crossed at 42±5 years (**Figure 2B**). This indicates that a major expression switch in skeletal muscles occurs during the first half of the fifth decade. This observation is in agreement with physiological studies in continuous cross-sectional cohorts showing that aging-related changes in muscle strength start between 40 to 50 years (Kirkwood, 2005; Lexell et al., 1988; Lindle et al., 1997; Sahin and Depinho, 2010). The aging-regulated genes were mapped to a wide spectrum of Kyoto Encyclopaedia of Genes and Genomes (KEGG) functional pathways.

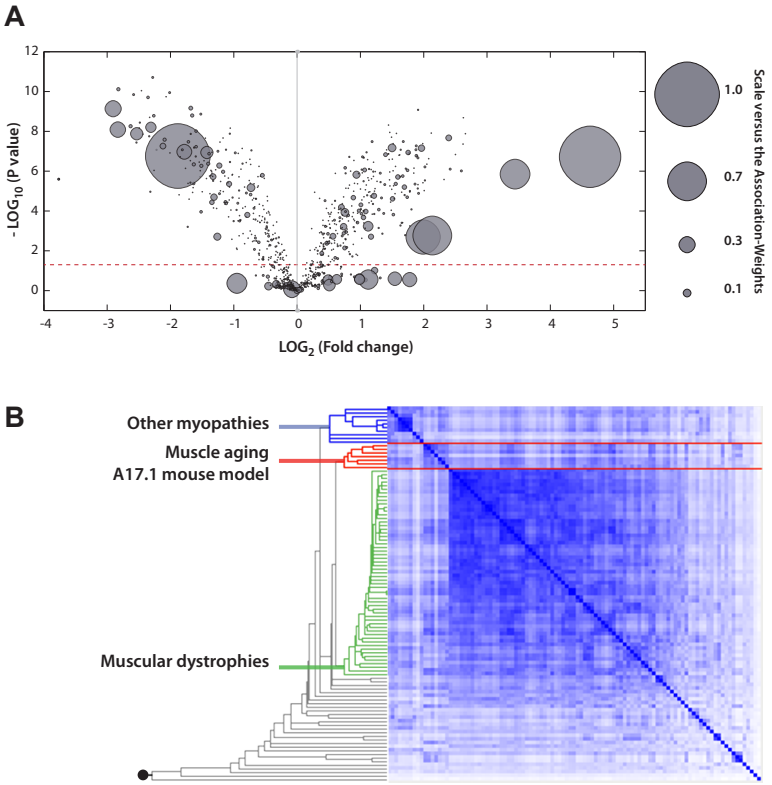

Figure 1 - The A17.1 mouse transcriptome is strongly associated with aging. A) Volcano plot shows the distribution of significantly deregulated genes (P = 0.05; indicated with a dashed line) in 6 week-old A17.1 mice against fold change. Genes are weighted based on their association with the *Aging* concept. The normalized association-weight is presented with a circle on a scale between 0.05 and 1, where 1 equals the highest association. **B)** Hierarchical clustering arrangements of 104 datasets in a literature-aided meta-analysis. Shades of blue indicate degree of similarities: from weak (white) to strong (dark blue). Three skeletal muscle aging-related datasets are clustered with OPMD dataset of 6 week-old mice (highlighted in red). The clusters associated with muscular dystrophies and other myopathies are highlighted in green and blue, respectively.

These aging-regulated KEGG pathways were highly similar to those that were identified from independent microarray study of skeletal muscles from two-age group (Welle et al., 2004; Welle et al., 2003; **Supplementary Table 2**).

Around midlife, muscle weakness symptoms are found in OPMD but not in age-matching controls (van der Sluijs et al., 2003) or in expPABPN1 carriers at a pre-symptomatic stage (**Supplementary Table 2**). OPMD-deregulated or pre-symptomatic-deregulated genes were identified from age-matching controls. Despite the limited number of samples in OPMD, OPMD-deregulated genes were highly similar to those identified in OPMD animal models (Anvar et al., 2011; Raz et al., 2011b). In OPMD large transcriptional changes were identified, but only minor transcriptional changes was identified at the pre-symtomatic stage (**Figure 2C**). Only 9% of the OPMD-deregulated genes were also deregulated in the pre-symptomatic (**Figure 2C**). 30 KEGG pathways were enriched in OPMD-deregulated genes (**Supplementary Table 2**), whereas no con-

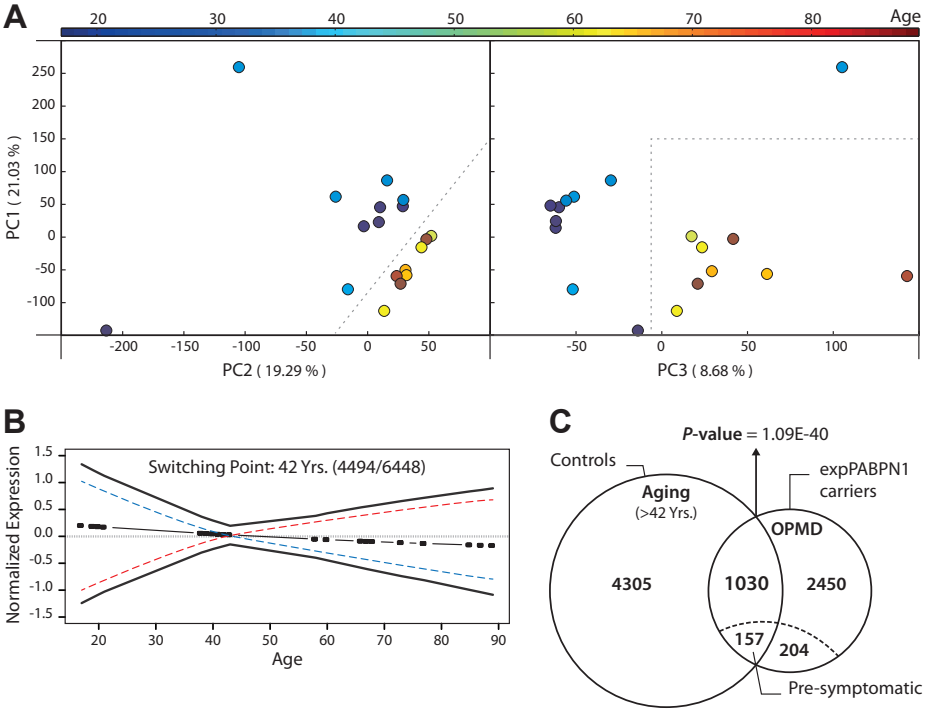

Figure 2 - High similarities between transcriptomes of muscle aging and OPMD. A) Principal component analysis (PCA) plots of skeletal muscle datasets from healthy controls (age is indicated with a colour scale). An age-associated variation is found with the first three principal components. Plots show sample distribution in the first and second (left) or first and third (right) components. The percentage of variations is indicated between brackets. The colour scale reflecting the age of the patient samples is given on top of the figure. Dashed lines separate samples into two age groups. **B)** Plot shows expression trends for the major cluster of 6448 probes whose expression are significantly changed with age (P<0.05). 4494 probes whose expression significantly change with age (p<0.05) were used for k-mean clustering analysis. Similar trends with up- and or down-regulation were combined using absolute correlation, revealing a switching point at 42±5 years. Up- or down- regulated expression trends (red and blue, respectively) are indicated with dashed lines, and continuous lines show the 95% boundaries. The middle line indicates the centroid with the age of individual samples. **C)** Venn diagram shows the overlap of between genes associated with aging (>42) and differentially expressed genes between OPMD- or expPABPN1 carriers and age-matched controls. Differentially expressed genes (P<0.05) in OPMD and pre-symptomatic carriers were identified from age matching control groups. P-values for overlap in differentially expressed genes were calculated with Fisher's exact test.

sistently deregulated KEGG pathways were found at the pre-symptomatic stage. This indicates that major transcriptional changes are associated with symptoms and age but not with the expression of expPABPN1 *per se*.

The transcriptional changes in OPMD were significantly similar to aging-regulated genes ($P = 1.1\times10^{-40}$; **Figure 2C**), and high similarity was also found between OPMD-deregulated and aging-regulated KEGG pathways from two independent studies (**Supplementary Table 2**). These analyses suggest that in both OPMD and muscle aging the major age-associated transcriptional changes occur during the fifth decade. These transcriptional changes are significantly similar. However, muscle weakness is found in OPMD and not in age-matching controls. This suggests

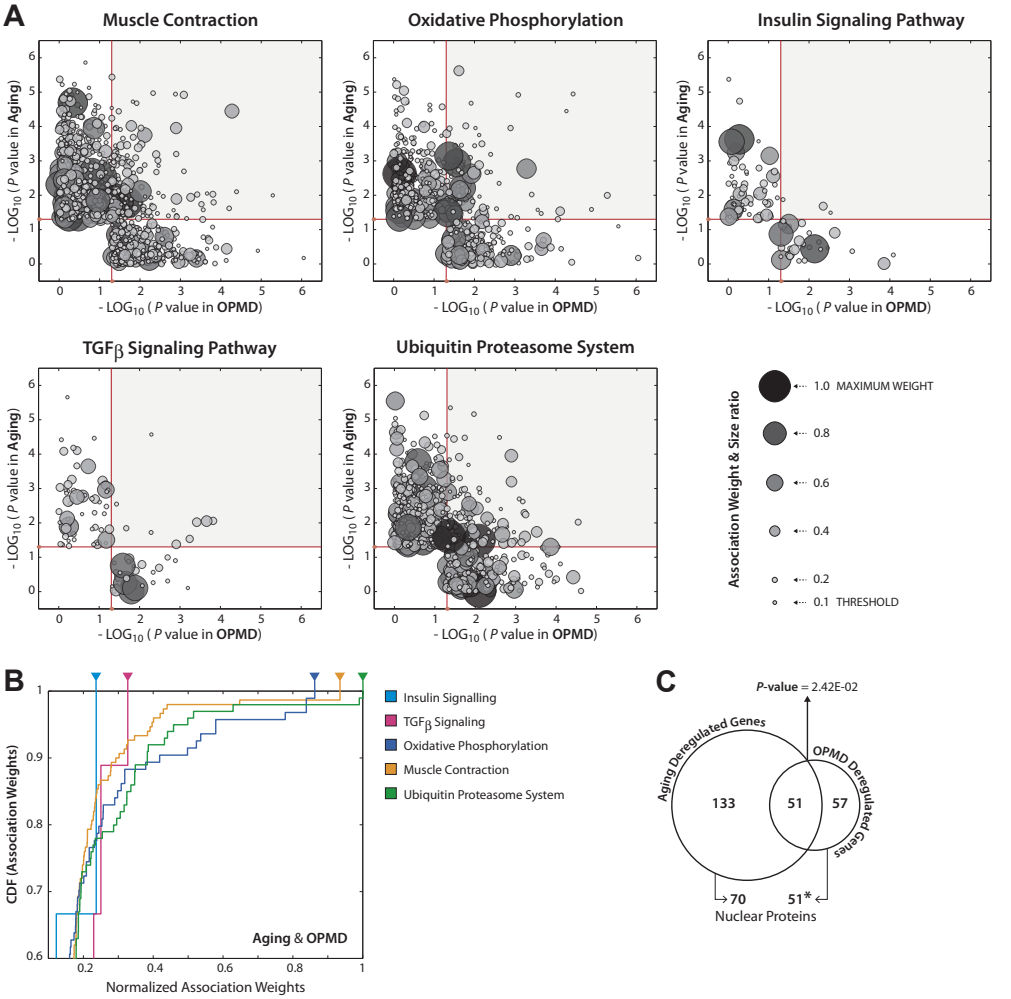

Figure 3 – Analysis of differentially expressed genes in aging and in OPMD reveals that the UPS is the most prominently associated biological process. A) 2D plots of selected biological processes, which are affected in both OPMD (x-axis) and muscle aging (y-axis). Significantly affected genes have *P*-value<0.05 (indicated with red lines). Gene association with 'muscle contraction', 'oxidative phosphorylation', 'insulin signalling pathway', 'TGFβ signalling pathway', and 'ubiquitin-proteasome system' terms is presented by a circle size. Normalized association weights < 0.1 are discarded. **B)** Cumulative distribution function (CDF) plots show the distribution of normalized association weights for overlapping deregulated genes between OPMD and muscle aging (>42 years) for each of the terms in **A**. Arrowheads indicate the maximum association weights.

that progression and or amplitude of those transcriptional changes may underlie differences in between OPMD and controls.

The UPS is the most affected pathway in OPMD and muscle aging

Next, we investigated the similarities of molecular changes in OPMD and aging-associated biological pathways using a literature-association study (LAS). In this study, we assessed the association weights of overlapping genes between muscle aging and OPMD with the five most robust

aging and OPMD-related pathways: oxidative phosphorylation, insulin signaling, tumor growth factor (TGFβ) signaling, the ubiquitin proteasome system (UPS) and muscle contraction (**Supplementary Table 2**). In the muscle contraction group, the overlapping genes between OPMD and muscle aging had high association weights (**Figure 3A**). This suggests that similar molecular signatures of muscle contraction are found in OPMD and muscle aging. The overlapping genes between OPMD and muscle aging were strongly associated with oxidative phosphorylation and the UPS (**Figure 3A**), while little similarity was found for highly influenced genes in the insulin or TGFβ signaling pathways (**Figure 3A**). This suggests that different key components in insulin or TGFβ signaling pathways are deregulated in OPMD and muscle aging.

The association weights of the overlapping genes in OPMD-deregulated and aging-regulated with five functional groups were ranked in Cumulative Distribution Function (CDF) plots and compared against a theoretical random distribution. The associations of the genes with UPS, oxidative phosphorylation and muscle contraction were much stronger than expected by chance (**Figure 3B**; Kolmogorov-Smirnov test: $P = 4.3\times10^{-39}$, 8.1×10^{-25} and 2.4×10^{-26}, respectively). In contrast, the distribution of association weights for genes in the insulin and TGFβ pathways were insignificant and did not differ from a theoretical random distribution. The low *P* value is, in part, due to the limited number of overlapping genes between OPMD and aging muscle in the latter pathways. The UPS ranked the highest suggesting that key components of the UPS contribute to both muscle aging and OPMD.

Age- related transcriptional changes are accelerated in OPMD

Clinical muscle weakness in quadriceps is found in OPMD patients but not in age-matching controls (**Supplementary Table 2**). Muscle weakness in quadriceps among healthy subjects is significant in the elderly (Hairi et al., 2010). Therefore, we investigated whether age-dependent expression changes are accelerated in OPMD compared to healthy individuals. Age-dependent expression trends of the probes that differentially expressed in both OPMD and aging were clustered using k-means clustering. One cluster of up- and one cluster of down-regulated probes in aging show earlier and accelerated changes in OPMD carriers (**Figure 4A**). Examples of reprehensive expression trends of individual genes from each cluster are presented in Figure 4B. Among those we identified the cell cycle regulator, *CDKN1A* (p21), and *LMOD1* and *CHRNA1* that are associated with muscle contraction. Among the genes with accelerated expression trends in OPMD, for some the expression is changed at the pre-symptomatic stage. This analysis suggests that expression trends in OPMD change faster compared with controls, and therefore changes in expression profiles are accelerated in OPMD.

Next we evaluated similarities in expression profiles between OPMD and elderly (>80 years). Significant overlap was identified between OPMD-deregulated and elderly-regulated genes ($P = 1.6\times10^{-168}$; **Figure 5A**). From those, 74% showed a similar direction of deregulation. Examples of genes with similar direction of deregulation in both datasets are shown in **Figure 5B**. All genes were identified as aging-regulated in independent studies (Welle et al., 2004; Lu et al., 2004; Rodwell et al., 2004). Since muscle weakness and atrophy is evident in elderly, this analysis suggests that similar molecular changes are associated with muscle weakness in OPMD and elderly.

We also investigated the pool of overlapping genes between OPMD and elderly. The relevance of this gene pool to aging was assessed with the literature concept 'Aging'. The association-weight of these genes to 'Aging' was very strong (**Figure 5C**). This confirms that this procedure can robustly and quantitatively identify gene association to literature concepts. Similar to the pool of overlap-

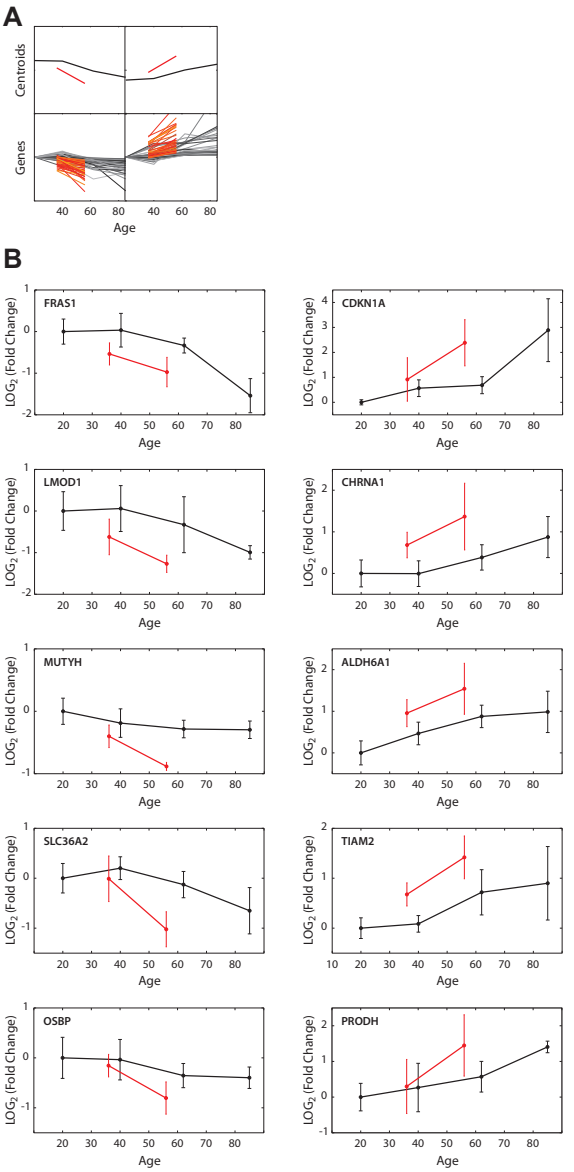

Figure 4 – Aging-associated expression trends are accelerated in OPMD. A) Expression trends of aging (>42)-regulated and OPMD-deregulated probes show progressive transcriptional changes in aging healthy controls (grey lines) and accelerated changes in OPMD (red lines). Upper plots show a summary trend (centroids) of all genes in each cluster, and lower plots show individual genes. **B)** Examples of expression trends of 10 genes from clusters in **A**, in healthy controls (grey lines) and in exPABPN1 carriers at pre-symptomatic and symptomatic stages (red lines). Standard deviations are indicated. Left and right columns show down- or up- regulated expression trends, respectively.

ping genes between aging and OPMD, in the OPMD-elderly pool, strong association was found with oxidative phosphorylation, the UPS and muscle contraction. The association with insulin and TGFβ signalling pathways was less strong (**Figure 5C**).

Protein homeostasis is mainly regulated by the autophagy-lysozyme system and the UPS. Since the UPS ranks the highest in both OPMD-aging and OPMD-elderly pool of genes, we next compared the association-weights of genes associated with lysozyme, autophagy and the UPS in the pool of OPMD-elderly overlapping genes. In contrast to the UPS, the association strength for autophagy and lysosome was very low (**Figure 5C**). The UPS was identified as the most significantly and consistently deregulated pathway in OPMD and models (Anvar et al., 2011). In that study deregulation of genes in autophagy and lysozyme ranked much lower and was not consistently significant in all OPMD model systems. This suggest that deregulation of genes in the UPS has the highest contribution to muscle weakness in both aging and OPMD.

PABPN1 expression progressively declines with aging and the decline is accelerated in OPMD

OPMD is caused by expression of exp-PABPN1. In the mouse model for OPMD severity of muscle weakness is associated with an increase in aggregates (Davies et al., 2005; Trollet et al., 2010). In models for OPMD aggregation depends on expression level. To our surprise, among the OPMD-deregulated genes in our microarray study we noticed PABPN1. To validate the microarray observation PABPN1 expression levels were determined with RT-qPCR of RNA from *Vastus lateralis*. Expression levels in OPMD patients or expPABPN1 carriers at the pre-symptomatic stage were compared

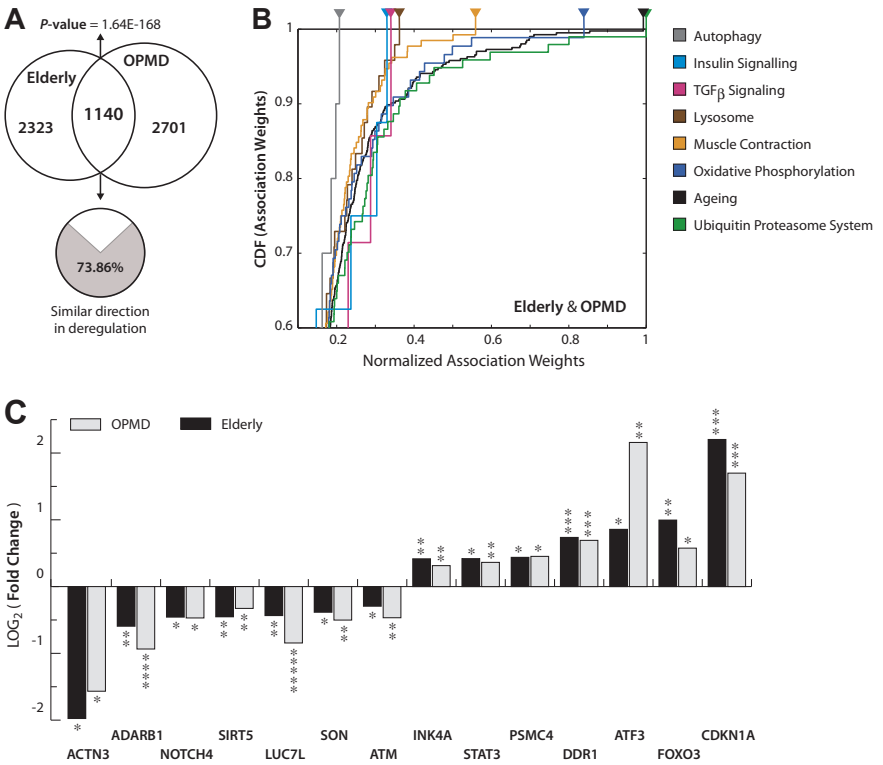

Figure 5 – Similar changes in expression between elderly and OPMD. A) Venn diagram shows the overlap of differentially expressed genes in OPMD- and in elderly (>80 year). From the 1140 overlapping genes, 77% show changes in a similar direction. The P-value for the overlap was calculated with Fisher's exact test. **B)** Histogram show change in expression levels of genes with significantly changed expression in the elderly (80 *vs.* 60 years) and in OPMD patients (*vs.* age-matched controls). All genes are reported in the literature as aging-deregulated (* P <0.05, ** P <0.005, *** P <0.0005, and **** P <0.00005). **C)** Cumulative distribution function (CDF) plots show the distribution of normalized association weights for overlapping deregulated genes between OPMD and elderly (>80 years) for each of the terms indicated in the figure. Arrowheads indicate the maximum association weights.

with age-matching control groups. A significant decline in expression was found in OPMD compared with age-matching controls (**Figure 6A**). At the pre-symptomatic stage a slight but insignificant reduction was found (**Figure 6A**). Since OPMD samples are significantly older compared with pre-symptomatic, we next analysed whether a change in PABPN1 expression level is associated with age. RT-qPCR was performed on *Vastus lateralis* from 78 healthy controls aged 17-89. A significant decline in *PABPN1* expression was identified from 43 years onwards (**Figure 6B**). A quadratic model or two linear models describes most accurately the change in PABPN1 expression during age (**Figure 6B**). A significant shift in expression was identified around 43 years (**Table 1**). This age-associated change in *PABPN1* expression shows a similar trend as decline in skeletal muscle strength during aging (Kent-Braun et al., 2002; Roth et al., 2002), which is initiated around midlife and progressively declines onwards. This suggests that changes in PABPN1 expression marks muscle aging. Moreover, symptoms in OPMD, but not the expression of exp-PABPN1 *per se,* are associated with a decline in *PABPN1* expression.

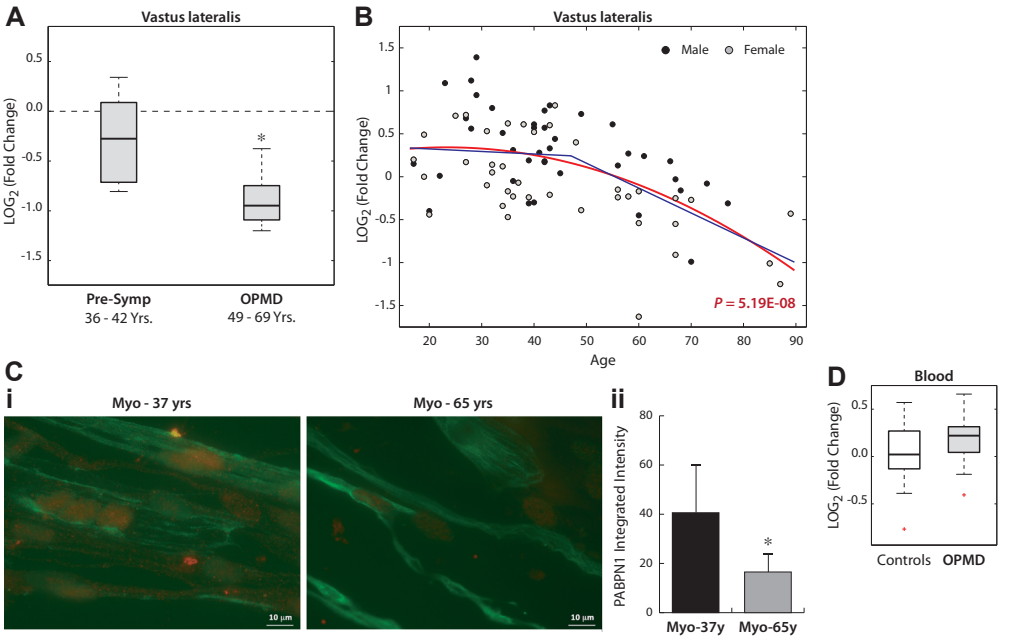

Figure 6 – PABPN1 expression declines in OPMD and during muscle aging. A) Box plot shows *PABPN1* LOG2 fold change in *Vastus lateralis*. Fold change was measured from RT-qPCR and was normalized to *GAPDH* and HRPT genes and to age matching control groups ($N_{pre\text{-}symptomatic}$ = 6, $N_{age\text{-}matched\ control\ group}$ = 16; N_{OPMD} = 9. $N_{age\text{-}matched\ control\ group}$ = 20). **B)** Scatter plot shows *PABPN1* LOG2 expression in quadriceps of 78 healthy controls between 17 and 89 years. Male and female samples are indicated in black and gray, respectively. A quadratic fit is shown with a red line (age 17-89), gender-corrected *P-value* for the quadratic fit is indicated in red. Blue dashed lines show linear fits for the age groups: 17 - 42 and 43 - 89 years. **C)** PABPN1 protein expression in primary myoblasts from young (37y) and old (65y) donors. **i)** Immunofluorescence of PABPN1 (red) and Desmin (green) in myotube cultures of 37 or 65 year-old donors. Scale bar is 10 mm. **ii)** Histogram shows integrated fluorescence intensity of PABPN1 in myonuclei of 37y and 65y cultures, N_{37y} = 103 and N_{65y} = 87 myonuclei. P value was calculated with the student's T-test, significant difference ($p<0.05$) is indicated with an asterisk. **D)** Box plot shows *PABPN1* LOG2 expression in blood of OPMD patients (N_{OPMD} = 16) and age-matched controls ($N_{age\text{-}matched\ control\ group}$ = 12). Expression values were normalized to *GAPDH* and HRPT genes.

To validate the decline in *PABPN1* mRNA expression, PABPN1 protein accumulation was determined in primary muscle cell cultures from 37 or 65 year-old individuals (**Figure 6C**). Protein analysis was performed on cultures that were in vitro propagated for a single passage. A nuclear staining of PABPN1 was found in these myoblasts. A decline in PABPN1 protein accumulation was observed in Myo-65y compared with Myo-37y, whereas the intensity of Desmin staining was unchanged (**Figure 6Ci**). Quantification of nuclear PABPN1 fluorescence intensity in myonuclei of fused myotubes revealed a significant decrease in Myo-65y compared with Myo-37y (**Figure 6Cii**).

PABPN1 is expressed in every cell whilst symptoms in OPMD are predominantly exhibited in a subset of skeletal muscles. To investigate whether the decline in PABPN1 expression is tissue specific, the expression of *PABPN1* was determined in blood samples of OPMD patients. RT-qPCR analysis revealed that *PABPN1* expression levels were unchanged between OPMD patients and age-matching controls (**Figure 6D**). This suggests that a decline in PABPN1 expression in OPMD

Table 1 – Changes in PABPN1 expression depends on chronological age are muscle specific.

Tissue	**Age** (years)	Beta	P-value
Vastus lateralis	17 – 42 (N = 41)	-0.006 (0.009)	0.37
	43 – 89 (N = 34)	-0.029 (0.006)	<0.0001
Frontal Brain Cortex	26 – 69 (N = 17)	0.002 (0.007)	0.73
	70 – 95 (N = 13)	-0.018 (0.008)	0.04
Blood	42 – 102 (N = 150)	0.001 (0.003)	0.69
Kidney Cortex	27 – 92 (N = 72)	-0.001 (0.002)	0.76
		-0.001 (0.002)	0.42
		-0.003 (0.002)	0.15
Kidney Medulla	29 – 92 (N = 61)	-0.003 (0.002)	0.11
		0.001 (0.002)	0.76
		-0.004 (0.002)	0.06
Rectus Abdominis	24 – 83 (N = 81)	-0.000 (0.003)	0.94
		0.010 (0.007)	0.13
		0.001 (0.003)	0.64
Parotid glands	19 – 71 (N = 13)	0.000 (0.003)	0.93
		0.003 (0.005)	0.64
		-0.001 (0.005)	0.86

Betas (standard errors of the mean) of a linear model are provided per probes. Values for three independent PABPN1 probes are shown for datasets from Kidney cortex, Kidney medulla, Rectus Abdominis and Partotid glands. *P-values* are adjusted for gender. Significant changes are highlighted in bold. N indicates number of samples. Age is indicates in years (y).

is muscle-specific. Next we investigated PABPN1 expression in several aging-related microarray studies from different tissues. A change in PABPN1 expression was not found in Blood, Parotid glands, kidney cortex or kidney medulla (**Table 1**). In postmortal frontal brain cortex we identified a small decline in PABPN1 expression in elderly (**Table 1**). Compared with PABPN1 decline in *Vastus lateralis*, the decline in the brain cortex was smaller and delayed (**Table 1**). Also in *Musculus rectus abdominis* PABPN1 expression was not changed with age (**Table 1**). *Rectus Abdominis* is a typical posture skeletal muscle, while the *Vastus lateralis* is involved in muscle movement. Moreover, muscle weakness is more pronounced in the *Vastus lateralis* compared with *Rectus Abdominis* (Marzani et al., 2005). Together, this analysis suggests that the age-associated decline in PABPN1 expression marks physiological aging in a subset of skeletal muscles.

PABPN1 down-regulation in human muscle cell culture induces cellular senescence and myogenic defects

To investigate the effect of PABPN1 down-regulation in muscle cells, three PABPN1 shRNA clones were selected for functional studies in immortalized human myoblast cultures using the lentivirus expression system. Compared with controls (H1 empty vector and non-transduced cells), the three PABPN1 shRNA clones, 121, 122 and 123, led to a 70%, 40% and 20% decrease in *PABPN1* expression (**Figure 6A**). These clones were selected as they represent a physiological decline in PABPN1. The sh121 clone led to down-regulation that is comparable to the decline in OPMD patients, while the sh122 clone led to a decline as in healthy controls around 60-70 years. The small decline in the sh123-transduced cells was comparable to the expression level in 40-50 year-old controls. Western blot analysis of protein extracts from fused cells confirmed substantial PABPN1 down-regulation in the sh121-transduced cell cultures, and about 40% reduction in

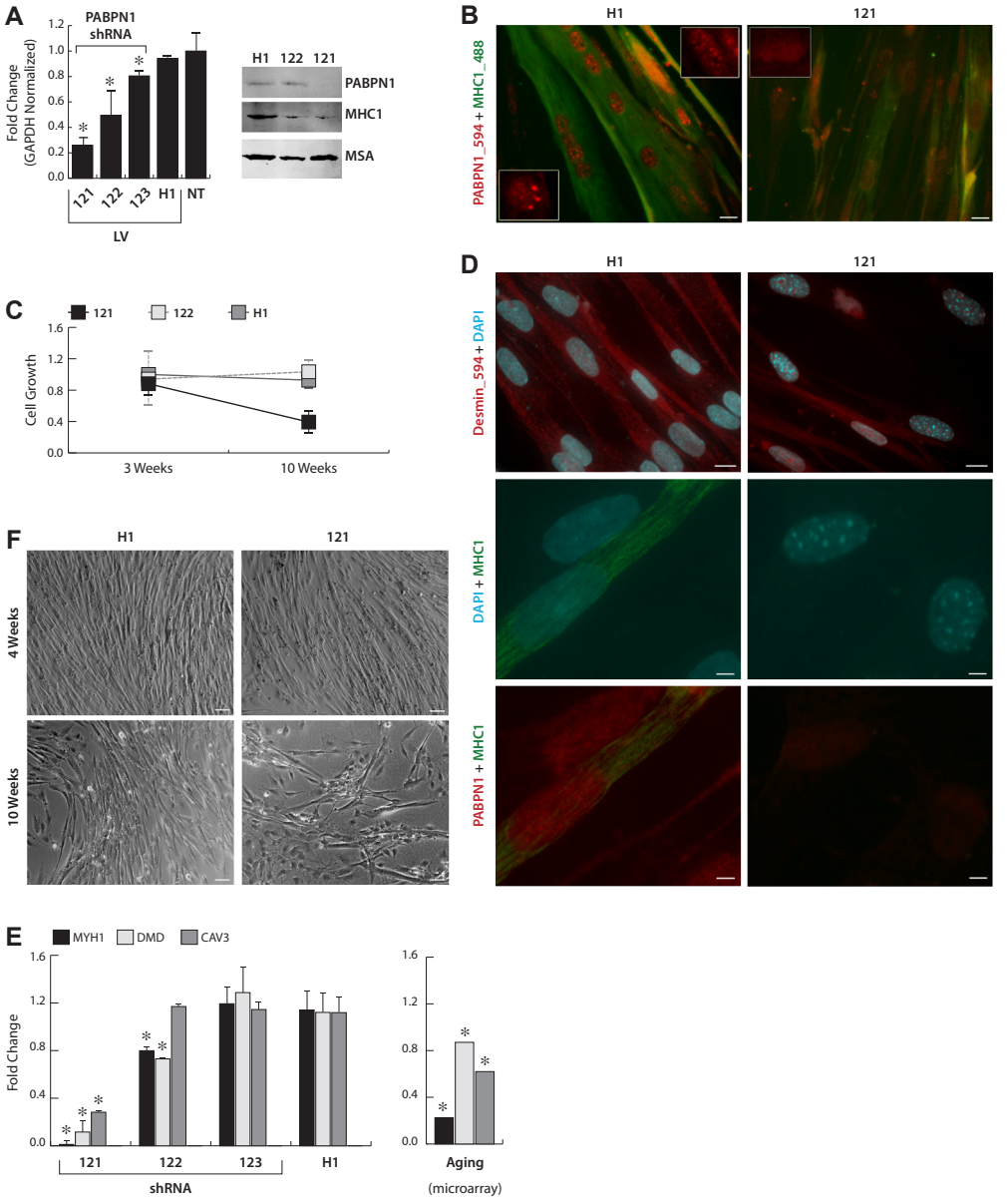

Figure 7 – PABPN1 down-regulation in myotubes shows myogenic defects and cell senescence. Human myotubes were transduced with shRNA specific to PABPN1 (121, 122, and 123) or H1 empty vector. Non-transduced (NT) cells were used as controls. **A)** Histograms show *PABPN1* expression in myoblasts two weeks after transduction. Fold change was normalized to *GAPDH* gene and to non-transduced cells. Averages are of 6 biological replicates. Western blot analysis of PABPN1, MHC1 and MSA in 121-, 122- or H1- transduced myotubes two weeks after transduction. **B)** Immunofluorescence of PABPN1 (labelled with Alexa-594) and myosin (labelled with Alexa-488) in 121- or H1-transduced fused myoblast cultures. Scale bars are 20 mm. A magnification of a single nucleus is shown in the boxed image. **C)** Cell growth analysis of 121-, 122- and H1- transduced myoblasts 3 or 10 weeks in culture. 50,000 cells were plated and were counted after 2 days in culture. Plots show normalized cell number to un-transduced controls. Averages are of 3 biological replicates. **D)** Left: Immunofluorescence of myotube cell cultures of desmin, PABPN1 and

MHC1. Cells were cultured for 10 weeks before fusion. Nuclei were counter stained with DAPI. Scale bars are 15 mm (Desmin) or 5 (PABPN1 and MHC1) mm. **E)** Images of fused myoblast H1- or 121- transduced cultures. Preceding fusion cells were maintained for 4 or 10 weeks after transduction. Scale bar is 30 mm. **F)** Left histogram shows RNA expression of *MYH1*, *DMD*, and *CAV3* in 121-, 122-, 123-, and H1-transduced fused myoblast cultures. Cells were cultured for 3 weeks before fusion. Fold change was normalized to *GAPDH* and to non-transduced cells. Averages are of 3 biological replicates. Significant down-regulation ($P<0.05$) is indicated with asterisks. Right histogram shows Fold change in the microarray study in aging.

sh122-transduced cells (**Figure 7A**). A decrease in the accumulation of nuclear PABPN1 was also verified by immunofluorescence in the sh121-transduced cells. A reduced PABPN1 signal was found in sh121 cells compared with control cells (**Figure 6B**). Nuclear PABPN1 is localized to speckles (Tavanez et al., 2005). In myonuclei of sh121 the speckle localization of PABPN1 was disrupted (**Figure 7B**, box). Together, this demonstrates that shRNAs for PABPN1 induced a decline in mRNA and protein accumulation.

Next we investigated cellular effects of PABPN1 down-regulation. Cell growth was not significantly affected in all myoblast cultures two or three passages after transduction (**Figure 7C**). However, after a longer culturing period, a 60% decline in cell growth was found in the sh121-transduced cells, whereas changes were not found in sh122, sh123-transduced cells or in controls (**Figure 7C**). Senescent cells are marked by heterochromatic foci (HF) (Spector and Gasser, 2003). We observed HF in the sh121-transduced cells but not in controls (**Figure 7D**). PABPN1 expression was undetectable in nuclei with HF (**Figure 7D**). In vivo, the majority of muscle cells are post-mitotic; therefore we compared the abundance of HF nuclei between myoblast and myotube cultures. 24% of myonuclei in 121-fused cultures contained HF whereas in 121-myoblasts only 9% of the cells were with HF. This suggests that the effect of PABPN1 down-regulation on cellular senescence is more pronounced in post-mitotic cells. Senescent muscle cells exhibit reduced fusion (Bigot et al., 2008). The fusion index in control cells was around 70% in transduced cells and controls, and was not significantly affected during in vitro propagation (**Figure 7E**). However, during in vitro propagation of the sh121-transduced cells cell fusion was reduced to 30% (**Figure 7E**). In concordance with cell growth, no significant reduced cell fusion was found in sh122- or sh123- transduced cells. Fusion defects can be associated with reduced expression of sarcomere encoding genes. RT-qPCR of *MYH1*, *DMD* and *CAV3* revealed a significant reduction in fused cultures of sh121-transduced cells (**Figure 7F**). For these genes a significant decline in expression was found in our microarray study (**Figure 7**). The decline in *MHY1* on mRNA level was consistent with a reduced protein accumulation in myotubes (**Figure 7A**). In the sh122- and sh123- transduced cells a gradual decrease in the expression of *MYH1* was observed, which corresponds to the decline in *PABPN1* expression (**Figure 7F**). The expression of *DMD* was significantly affected in the sh122- but not in the sh123- transduced cells. The expression of *CAV3* reduced only in the sh121-transduced cells. Our experiments in this cell model suggest a regulatory role for PABPN1 expression level in induction of cell senescence in muscle cells, which is associated with a gradual change in expression of sarcomeric genes.

DISCUSSION

PABPN1 regulates poly(A) tail length and mRNA stability (Lemay et al., 2010; Kuhn et al., 2009), and thus plays an indispensable role in cell homeostasis by affecting genome-wide mRNA accumulation. Previous studies demonstrated that a complete knockdown of PABPN1 causes shorting of poly(A) tail, which is associated with myogenic defects, including reduction in cell growth and fusion (Apponi et al., 2010; Chartier et al., 2006; Davies et al., 2006; Trollet et al., 2010). Here, for the first time, a significant decline of PABPN1 expression in affected muscles of OPMD patients is

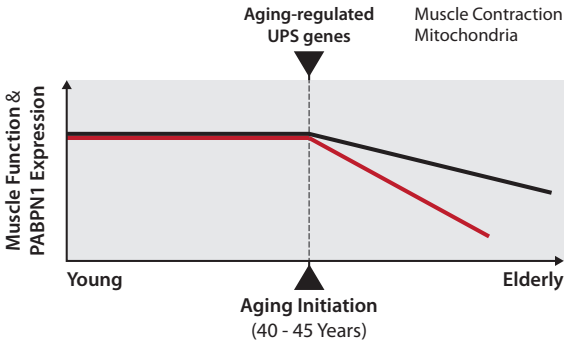

Figure 8 – Schematic presentation of decline in PABPN1 expression in association with protein aggregation during aging. Upper panel represents age-associated changes in PABPN1 expression manifested during midlife, with acceleration in OPMD (in red). Lower panel illustrates the decline in the level of soluble PABPN1 during aging of skeletal muscle, regulated by the UPS.

reported. Since a decline in PABPN1 expression was not found at the pre-symptomatic stage it suggests that the decline in PABPN1 expression is not caused by the expression of expPABPN1, *per se*. We show that a down-regulation of PABPN1 expression, to levels that are found *in vivo* (OPMD and aging), in muscle cell culture leads to cellular defects, including cell senescence and myogenic defects. In accordance with disease progression, the decline in cell growth and fusion correlates with levels of PABPN1 down-regulation. Primary myoblast cultures from OPMD patients also exhibit reduced cell growth and fusion defects (Perie et al., 2006). Overexpression of PABPN1 also leads to muscle cell defects and atrophy, which is associated with genome-wide transcriptional chances (Trollet et al., 2010). Mild overexpression of either expPABPN1 or the wild type allele in fused muscle cell culture also leads to transcriptional changes (Raz et al., 2011b). These changes, however, are significantly smaller compared with high overexpression situations (Raz et al., 2011b). Since PABPN1 regulates poly(A) length and hence mRNA stability, these studies together suggest that manipulations of PABPN1 expression levels below or above a narrow threshold leads to widespread transcriptional changes in muscle cells.

PABPN1 is ubiquitously expressed but symptoms in OPMD are predominately exhibited in a subset of skeletal muscles. Here we found that in OPMD PABPN1 expression declines in skeletal muscles but not in blood. During normal muscle aging, PABPN1 level also decreases. However, this decline is slower and smaller than in OPMD. The decline in PABPN1 expression was not found in other tissues like kidney, Parotid glands, blood or *Rectus Abdominis* muscles, which is less affected during aging. A smaller and delayed decline in PABPN1 was identified in brain cortex. This suggests that a decline in PABPN1 expression is more prominent in skeletal muscles. The decline was progressive from the age 43± years, and perfectly fit to the decline in muscle weakness during aging (Beenakker et al., 2010). Previous studies demonstrated significant muscle weakness in quadriceps of elderly (Kent-Braun et al., 2002; Roth et al., 2002). A major switch in expression profiles in both OPMD and aging was identified during the first half of the fifth decade. This suggests that similar mechanisms initiate muscle weakness in aging and OPMD. Transcriptional similarities between OPMD and elderly suggest differences in progression of aging-regulated muscle weakness between OPMD and normal aging (**Figure 8**).

Protein aggregation is the hallmark of OPMD. Both wild type and mutant PABPN1 are prone to aggregation. However, aggregation potency of expPABPN1 is higher than that of the wild type protein (Raz et al., 2011b). In contrast to the aggregation process of wild type PABPN1, that of expPABPN1 is irreversible and encompasses stable pre-aggregated forms or oligomers (Raz et al., 2011a). Aggregates of both wild type and expPABPN1 entrap a broad rage of nuclear proteins, including components of the UPS (Calado et al., 2000; Anvar et al., 2011). The rate of protein entrapment differs between aggregation process of wild type and mutant PABPN1 (Raz et al.,

2011a). Protein entrapment can be associated with transcriptional changes of nuclear proteins and UPS encoding genes (Corbeil-Girard et al., 2005; Anvar et al., 2011). Since proteostasis of nuclear proteins is predominantly regulated by the UPS, changes in expression of UPS encoding genes would affect the ratio of soluble to aggregated proteins. PABPN1 aggregation reduces the levels of soluble PABPN1 (Raz et al., 2011b), and therefore could lead to a similar effect as down-regulation. Aggregation of PABPN1 is regulated by the UPS (Raz et al., 2011b). Moreover, transcriptional changes of the UPS were identified in OPMD and aging. In elderly and OPMD the UPS ranked with a highest association. Functional decline of the UPS is associated with an accumulation and aggregation of misfolded proteins (Balch et al., 2008; Morimoto, 2008; Sherman and Goldberg, 2001). In *C. elegance*, aging is associated with widespread accumulation of aggregated proteins (David et al., 2010). Changes in proteasome activity in skeletal muscles were observed in muscle aging (Ferrington et al., 2005). We suggest that age-associated changes in UPS expression play a role in OPMD onset (**Figure 8**).

Altogether, our data reveals a strong association between PABPN1 expression in OPMD and in muscle aging. A decline in PABPN1 expression marks muscle aging and we suggest that PABPN1 plays an indispensable role in muscle homeostasis. From this study new regulators of aging cells could be identified in future studies.

MATERIALS AND METHODS

Human materials, RNA extraction and RT-qPCR

Datasets: Human and mouse samples that were used in the microarray studies have been previously published (Anvar et al., 2011; Trollet et al., 2010). A summary of human samples is listed in **Supplementary Table 1**.

All human muscle biopsies presented in this study were collected at Radboud Hospital, Nijmegen, Canisius-Wilhelmina Hospital, Nijmegen, The Netherlands, and Rigshospitalet, Denmark, after an approval of the medical ethical committee Arnhem-Nijmegen (CMO nr. 2005/189) and of the local ethical committee, from The NL and Denmark, respectively. OPMD patients and pre-symptomatic were genetically confirmed and underwent clinical investigation including MRC score prior to sampling of muscle biopsy. All quadriceps biopsies were collected using the Bergstrom needle procedure. The biopsies froze immediately in liquid nitrogen and stored at -80 before RNA extraction.

RNA extraction and RT-qPCR were performed as described in (Trollet et al., 2010). Expression levels were calculated according to the ΔΔCT method, and were first normalized to *GAPDH* housekeeping gene and then to controls (17 - 25 years) in the aging studies, or to the age-matching controls in the studies of expPABPN1 carriers. The statistical significance was determined with the Student's t-test. The list of primers used in this study is provided in **Supplementary Table 3**.

Microarray and Statistical Analyses

The human and mouse microarray datasets are publicly available at GEO repository under the accession numbers GSE26605 and GSE26604, respectively. In all datasets genome-wide expression profiles of skeletal muscles from OPMD were compared to controls. *PABPN1* expression in non-muscle tissues was identified from previously published microarrays, all are publically available: frontal cortex: (GEO-GD707, GEO-GSE1572; Lu et al., 2004), *Rectus abdominis* (GEO-GSE5086; Zahn et al., 2006), blood (GEO-GSE16717; Passtoors et al., 2012), kidney (Rodwell et al., 2004) and Parotid glands (GEO-GSE8764; Srivastava et al., 2008).

Data Processing: Quantile normalization was applied on the microarray raw dataset and data quality was assessed by the principal component analysis. Differentially expressed genes between two age-groups were identified by applying hierarchical linear model using limma package in R (Smyth, 2004) at a cut-off of 0.05. Furthermore, a list of aging-deregulated genes was filtered for those that could not be confirmed after integration with additional set of control individuals in an independent dataset. The OPMD-deregulated genes in the OPMD mouse model and patients were identified as previously described (Anvar et al., 2011; Trollet et al., 2010). Probe annotation was carried out using illuminaHumanv3BeadID (human) and illuminaMousev1BeadID (mouse) R packages. Statistical significance of gene overlap was carried out with the Fisher's exact test in R.

The principal component analysis (PCA) was applied on the human dataset to identify outliers and to investigate age-associated variations. PCA analysis was performed in Matlab and in R.

For the literature-aided study (LAS) the association weights between genes and each biological process were mined using Anni 2.1 (Jelier et al., 2008b). The association weights were normalized to the scale between 0 and 1, relative to the maximum association weight. Threshold of 0.1 was applied to remove genes with weak association (based on the level of evidential support in literature). In addition, genes with $P > 0.05$ ($-\log_{10} > 1.3$) in muscle aging and OPMD were excluded.

Cumulative Distribution Function (CDF) plots were used to examine the association distribution for deregulated genes in OPMD and muscle aging. The CDF of $Gene_i$ is defined as the proportion of genes with association weight less than or equal to that of $Gene_i$. The Kolmogorov-Smirnov (KS) test was used to identify distributions that significantly differ from a theoretical distribution, threshold of $P < 10^{-3}$. Statistical tests were performed in Matlab.

The k-means clustering was used to identify similar expression trends. The procedure was made with probes. For the control samples an absolute correlation was applied to cluster probes with reciprocal (up or down) trends. However, in order to optimize the clustering arrangements, average Silhouette (S_{avg}) values are calculated for each cluster in Matlab. Clustering arrangement of partitions with $S_{avg} < 0.6$ were reiterated until the criteria has met. Maximum number of clusters was set to 20 to avoid overly complex clustering arrangement due to the size of the set. The cluster centroids were used to provide summarized age-dependent expression patterns for each cluster.

Statistical analyses of linear and quadratic models were carried out with the SPSS software (IMB) and Matlab, and plots were generated in Matlab.

Pathway Analyses: Genes were mapped to KEGG pathways (Kyoto Encyclopedia of Genes and Genomes) for assessment of significant transcriptional deregulation in aging (>42 years) or in OPMD using global test (Goeman et al., 2004; Jelier et al., 2011). DAVID, a functional annotation clustering tool (Dennis, Jr. et al., 2003; Huang et al., 2009), was used for integration and removing redundancy. The previously published datasets of Welle et al. (Welle et al., 2004) were used for replication and independent confirmation of pathway analysis. Subcellular localization was carried out with Gene Ontology. A recent annotation of genes encoding for aggregation-prone proteins (David et al., 2010) was used to map the human homologues genes using HomoloGene (*http://ncbi.nlm.nih.gov/homologene*) and Inparanoid (*http://inparanoid.sbc.su.se*) online databases. The meta-analysis was carried out on 104 microarray datasets from various organisms as described in Jelier et al. (Jelier et al., 2008a).

Cell culture and Lentivirus transduction

The human 7304 immortalized myoblasts were a kind gift from Francesco Muntoni (University College London, UK) and were prepared by Gillian Butler-Browne and Vincent Mouly (Zhu et al., 2007). The 7304 cells were propagated in a medium containing DMEM+20% Fetal Calf Serum supplemented with an equal volume Skeletal Muscle Cell Media (PromoCell, Heidelberg, Germany) at 37 °C under 5% CO_2. Cell fusion was carried out in a medium containing DMEM+5% Horse Serum. Human skeletal primary myoblasts from a 37-year-old (37y) and a 65-year-old (65y) donor (Tebu-bio, Le Perray en Yvelines, France) are described in (Righolt et al., 2011). Cells were propagated for only one or two passages and subsequently were seeded on collagen-coated glass plates for imaging.

The shRNA in lentivirus expression vectors 121 (TRCN0000000121), 122 (TRCN0000000122) and (TRCN0000000123) 123 were obtained from Sigma-Aldrich. An empty vector, H1, was used as a negative control. Lentivirus particles were produced as described in (Raz et al., 2006). Virus transduction was performed with 2mg/ml polybrene. Cells were cultured with viruses (MOI ~25) overnight, followed by medium refreshing. Transduced cells were maintained in the presence of 5mg/ml puromycin. *PABPN1* down-regulation was determined 3 days, 4 weeks and 8 weeks after transduction using RT-qPCR. Down regulation did not change during culturing. In total, 4 independent transduction experiments were performed. Cell fusion and cell growth experiments

were carried out in the absence of puromycin. For cell growth analysis 50,000 cells were seeded in triplicates in a 24 well plate and the number of living cells was counted after two days with TC10™ Automated Cell Counter (BioRad Hercules, CA, USA). Cell growth experiments were carried out 3 and 10 weeks after transduction. Cell fusion was carried out 10 weeks after transduction in triplicates and cell fusion index was determined by dividing the number of nuclei in myotubes to the total number of myotubes.

Immunofluorescence and western blot analyses

The analysis of fused cells was carried out on cells seeded on plastics or on collagen-coated glass plates. Immunofluorescence was carried out as described in (Raz et al., 2006). Images were recorded as described in (Raz et al., 2011b). Primary antibodies used were: anti-Myosin MF20 (Sigma-Aldrich, MO, USA); anti-Desmin (1:500; Cell Signalling Technology, MS, USA) and the anti-PABPN1, 3F5 llama single chain antibody (1:1000; Verheesen et al., 2006), recognised with rabbit-anti-VHH (1:2000). The Alexa 488-, Alexa 430- or Alexa 594- conjugated secondary antibodies against primary antibodies were obtained from Molecular Probes (Invitrogen, CA, USA) and used (1:2000). DAPI (Sigma-Aldrich, MO, USA) was used for DNA counterstaining.

Western blot analysis of total proteins that were extracted from fused cells was carried out as described in (Raz et al., 2011b). Primary antibodies were mouse monoclonal anti-muscle actin (MSA) (1:2000) (Novocastra, Newcastle upon Tyne, UK), 3F5 llama single chain antibody (1:1000) recognised with rabbit-anti-VHH (1:2000) and anti-Myosin MF20 (1:500) (Sigma-Aldrich). Detection of the first antibodies was conducted with the Odyssey Infrared Imaging System (LI-COR Biosciences, NE, USA) and suitable secondary antibodies.

Acknowledgement

This work was funded in part by the European Commission (PolyALA LSHM-CT-2005018675) and Muscular Dystrophy Association (nr: 68016). Association Francaise contre les Myopathies (nr: 15 123) and the Centre for Medical Systems Biology within the framework of the Netherlands Genomics Initiative (NGI)/Netherlands Organisation for Scientific Research (NWO). The funders had no role in study design, data collection and analysis, decision to publish, or preparation of the manuscript.

Reference List

Abu-Baker,A., Messaed,C., Laganiere,J., Gaspar,C., Brais,B., and Rouleau,G.A. (2003). Involvement of the ubiquitin-proteasome pathway and molecular chaperones in oculopharyngeal muscular dystrophy. Hum. Mol. Genet *12*, 2609-2623.

Anvar,S.Y., 't Hoen,P.A., Venema,A., van der Sluijs,B., van,E.B., Snoeck,M., Vissing,J., Trollet,C., Dickson,G., Chartier,A., Simonelig,M., van Ommen,G.J., van der Maarel,S.M., and Raz,V. (2011). Deregulation of the ubiquitin-proteasome system is the predominant molecular pathology in OPMD animal models and patients. Skelet. Muscle *1*, 15.

Apponi,L.H., Leung,S.W., Williams,K.R., Valentini,S.R., Corbett,A.H., and Pavlath,G.K. (2010). Loss of nuclear poly(A)-binding protein 1 causes defects in myogenesis and mRNA biogenesis. Hum. Mol. Genet. *19*, 1058-1065.

Balch,W.E., Morimoto,R.I., Dillin,A., and Kelly,J.W. (2008). Adapting proteostasis for disease intervention. Science *319*, 916-919.

Beenakker,K.G., Ling,C.H., Meskers,C.G., de Craen,A.J., Stijnen,T., Westendorp,R.G., and Maier,A.B. (2010). Patterns of muscle strength loss with age in the general population and patients with a chronic inflammatory state. Ageing Res. Rev *9*, 431-436.

Benoit,B., Mitou,G., Chartier,A., Temme,C., Zaessinger,S., Wahle,E., Busseau,I., and Simonelig,M. (2005). An essential cytoplasmic function for the nuclear poly(A) binding protein, PABP2, in poly(A) tail length control and early development in Drosophila. Dev. Cell *9*, 511-522.

Berciano,M.T., Villagra,N.T., Ojeda,J.L., Navascues,J., Gomes,A., Lafarga,M., and Carmo-Fonseca,M. (2004). Oculopharyngeal muscular dystrophy-like nuclear inclusions are present in normal magnocellular neurosecretory neurons of the hypothalamus. Hum. Mol. Genet *13*, 829-838.

Bigot,A., Jacquemin,V., Debacq-Chainiaux,F., Butler-Browne,G.S., Toussaint,O., Furling,D., and Mouly,V. (2008). Replicative aging down-regulates the myogenic regulatory factors in human myoblasts. Biol. Cell *100*, 189-199.

Brais,B., Bouchard,J.P., Xie,Y.G., Rochefort,D.L., Chretien,N., Tome,F.M., Lafreniere,R.G., Rommens,J.M., Uyama,E., Nohira,O., Blumen,S., Korczyn,A.D., Heutink,P., Mathieu,J., Duranceau,A., Codere,F., Fardeau,M., and Rouleau,G.A. (1998). Short GCG expansions in the PABP2 gene cause oculopharyngeal muscular dystrophy. Nat Genet *18*, 164-167.

Brais,B., Xie,Y.G., Sanson,M., Morgan,K., Weissenbach,J., Korczyn,A.D., Blumen,S.C., Fardeau,M., Tome,F.M., Bouchard,J.P., and . (1995). The oculopharyngeal muscular dystrophy locus maps to the region of the cardiac alpha and beta myosin heavy chain genes on chromosome 14q11.2-q13. Hum. Mol. Genet *4*, 429-434.

Calado,A., Tome,F.M., Brais,B., Rouleau,G.A., Kuhn,U., Wahle,E., and Carmo-Fonseca,M. (2000). Nuclear inclusions in oculopharyngeal muscular dystrophy consist of poly(A) binding protein 2 aggregates which sequester poly(A) RNA. Hum. Mol. Genet *9*, 2321-2328.

Catoire,H., Pasco,M.Y., Abu-Baker,A., Holbert,S., Tourette,C., Brais,B., Rouleau,G.A., Parker,J.A., and Neri,C. (2008). Sirtuin inhibition protects from the polyalanine muscular dystrophy protein PABPN1. Hum. Mol. Genet. *17*, 2108-2117.

Chartier,A., Benoit,B., and Simonelig,M. (2006). A Drosophila model of oculopharyngeal muscular dystrophy reveals intrinsic toxicity of PABPN1. EMBO J *25*, 2253-2262.

Chartier,A., Raz,V., Sterrenburg,E., Verrips,C.T., van der Maarel,S.M., and Simonelig,M. (2009). Prevention of oculopharyngeal muscular dystrophy by muscular expression of Llama single-chain intrabodies in vivo. Hum. Mol. Genet. *18*, 1849-1859.

Corbeil-Girard,L.P., Klein,A.F., Sasseville,A.M., Lavoie,H., Dicaire,M.J., Saint-Denis,A., Page,M., Duranceau,A., Codere,F., Bouchard,J.P., Karpati,G., Rouleau,G.A., Massie,B., Langelier,Y., and Brais,B. (2005). PABPN1 overexpression leads to upregulation of genes encoding nuclear proteins that are sequestered in oculopharyngeal muscular dystrophy nuclear inclusions. Neurobiol. Dis. *18*, 551-567.

David,D.C., Ollikainen,N., Trinidad,J.C., Cary,M.P., Burlingame,A.L., and Kenyon,C. (2010). Widespread protein aggregation as an inherent part of aging in C. elegans. PLoS. Biol. *8*, e1000450.

Davies,J.E., Sarkar,S., and Rubinsztein,D.C. (2006). Trehalose reduces aggregate formation and delays pathology in a transgenic mouse model of oculopharyngeal muscular dystrophy. Hum. Mol. Genet *15*, 23-31.

Davies,J.E., Wang,L., Garcia-Oroz,L., Cook,L.J., Vacher,C., O'Donovan,D.G., and Rubinsztein,D.C. (2005). Doxycycline attenuates and delays toxicity of the oculopharyngeal muscular dystrophy mutation in transgenic mice. Nat Med. *11*, 672-677.

Dennis,G., Jr., Sherman,B.T., Hosack,D.A., Yang,J., Gao,W., Lane,H.C., and Lempicki,R.A. (2003). DAVID: Database for Annotation, Visualization, and Integrated Discovery. Genome Biol. *4*, 3.

Ferrington,D.A., Husom,A.D., and Thompson,L.V. (2005). Altered proteasome structure, function, and oxidation in aged muscle. FASEB J. *19*, 644-646.

Giresi,P.G., Stevenson,E.J., Theilhaber,J., Koncarevic,A., Parkington,J., Fielding,R.A., and Kandarian,S.C. (2005). Identification of a molecular signature of sarcopenia. Physiol Genomics *21*, 253-263.

Goeman,J.J., van de Geer,S.A., de,K.F., and van Houwelingen,H.C. (2004). A global test for groups of genes: testing associa-

tion with a clinical outcome. Bioinformatics. *20*, 93-99.

Hairi,N.N., Cumming,R.G., Naganathan,V., Handelsman,D.J., Le Couteur,D.G., Creasey,H., Waite,L.M., Seibel,M.J., and Sambrook,P.N. (2010). Loss of muscle strength, mass (sarcopenia), and quality (specific force) and its relationship with functional limitation and physical disability: the Concord Health and Ageing in Men Project. J. Am. Geriatr. Soc. *58*, 2055-2062.

Huang,d.W., Sherman,B.T., and Lempicki,R.A. (2009). Systematic and integrative analysis of large gene lists using DAVID bioinformatics resources. Nat Protoc. *4*, 44-57.

Jelier,R., 't Hoen,P.A., Sterrenburg,E., den Dunnen,J.T., van Ommen,G.J., Kors,J.A., and Mons,B. (2008a). Literature-aided meta-analysis of microarray data: a compendium study on muscle development and disease. BMC. Bioinformatics. *9*, 291.

Jelier,R., Goeman,J.J., Hettne,K.M., Schuemie,M.J., den Dunnen,J.T., and 't Hoen,P.A. (2011). Literature-aided interpretation of gene expression data with the weighted global test. Brief. Bioinform.

Jelier,R., Schuemie,M.J., Veldhoven,A., Dorssers,L.C., Jenster,G., and Kors,J.A. (2008b). Anni 2.0: a multipurpose text-mining tool for the life sciences. Genome Biol. *9*, R96.

Kent-Braun,J.A., Ng,A.V., Doyle,J.W., and Towse,T.F. (2002). Human skeletal muscle responses vary with age and gender during fatigue due to incremental isometric exercise. J. Appl. Physiol *93*, 1813-1823.

Kirkwood,T.B. (2005). Understanding the odd science of aging. Cell *120*, 437-447.

Kirkwood,T.B. and Austad,S.N. (2000). Why do we age? Nature *408*, 233-238.

Kuhn,U., Gundel,M., Knoth,A., Kerwitz,Y., Rudel,S., and Wahle,E. (2009). Poly(A) tail length is controlled by the nuclear poly(A)-binding protein regulating the interaction between poly(A) polymerase and the cleavage and polyadenylation specificity factor. J. Biol. Chem. *284*, 22803-22814.

Lemay,J.F., D'Amours,A., Lemieux,C., Lackner,D.H., St-Sauveur,V.G., Bahler,J., and Bachand,F. (2010). The nuclear poly(A)-binding protein interacts with the exosome to promote synthesis of noncoding small nucleolar RNAs. Mol. Cell *37*, 34-45.

Lexell,J., Taylor,C.C., and Sjostrom,M. (1988). What is the cause of the ageing atrophy? Total number, size and proportion of different fiber types studied in whole vastus lateralis muscle from 15- to 83-year-old men. J. Neurol. Sci. *84*, 275-294.

Lindle,R.S., Metter,E.J., Lynch,N.A., Fleg,J.L., Fozard,J.L., Tobin,J., Roy,T.A., and Hurley,B.F. (1997). Age and gender comparisons of muscle strength in 654 women and men aged 20-93 yr. J. Appl. Physiol *83*, 1581-1587.

Ling,C.H., Taekema,D., de Craen,A.J., Gussekloo,J., Westendorp,R.G., and Maier,A.B. (2010). Handgrip strength and mortality in the oldest old population: the Leiden 85-plus study. CMAJ. *182*, 429-435.

Liu,C.J. and Latham,N. (2011). Can progressive resistance strength training reduce physical disability in older adults? A meta-analysis study. Disabil. Rehabil. *33*, 87-97.

Lu,T., Pan,Y., Kao,S.Y., Li,C., Kohane,I., Chan,J., and Yankner,B.A. (2004). Gene regulation and DNA damage in the ageing human brain. Nature *429*, 883-891.

Marzani,B., Felzani,G., Bellomo,R.G., Vecchiet,J., and Marzatico,F. (2005). Human muscle aging: ROS-mediated alterations in rectus abdominis and vastus lateralis muscles. Exp. Gerontol. *40*, 959-965.

Morimoto,R.I. (2008). Proteotoxic stress and inducible chaperone networks in neurodegenerative disease and aging. Genes Dev. *22*, 1427-1438.

Passtoors,W.M., Boer,J.M., Goeman,J.J., Akker,E.B., Deelen,J., Zwaan,B.J., Scarborough,A., Breggen,R., Vossen,R.H., Houwing-Duistermaat,J.J., Ommen,G.J., Westendorp,R.G., Heemst,D., Craen,A.J., White,A.J., Gunn,D.A., Beekman,M., and Slagboom,P.E. (2012). Transcriptional profiling of human familial longevity indicates a role for ASF1A and IL7R. PLoS. One. *7*, e27759.

Perie,S., Mamchaoui,K., Mouly,V., Blot,S., Bouazza,B., Thornell,L.E., St Guily,J.L., and Butler-Browne,G. (2006). Premature proliferative arrest of cricopharyngeal myoblasts in oculo-pharyngeal muscular dystrophy: Therapeutic perspectives of autologous myoblast transplantation. Neuromuscul Disord *16*, 770-781.

Raz,V., Abraham,T., van Zwet,E.W., Dirks,R.W., Tanke,H.J., and van der Maarel,S.M. (2011a). Reversible aggregation of PABPN1 pre-inclusion structures. Nucleus. *2*, 208-218.

Raz,V., Carlotti,F., Vermolen,B.J., van der,P.E., Sloos,W.C., Knaan-Shanzer,S., de Vries,A.A., Hoeben,R.C., Young,I.T., Tanke,H.J., Garini,Y., and Dirks,R.W. (2006). Changes in lamina structure are followed by spatial reorganization of heterochromatic regions in caspase-8-activated human mesenchymal stem cells. J Cell Sci. *119*, 4247-4256.

Raz,V., Routledge,S., Venema,A., Buijze,H., van der Wal,E., Anvar,S.Y., Straasheijm,K.R., Klooster,R., Antoniou,M., and van der Maarel,S.M. (2011b). Modeling Oculopharyngeal Muscular Dystrophy in Myotube Cultures Reveals Reduced Accumulation of Soluble Mutant PABPN1 Protein. Am. J. Pathol.

Righolt,C.H., van 't Hoff,M.L., Vermolen,B.J., Young,I.T., and Raz,V. (2011). Robust nuclear lamina-based cell classification of aging and senescent cells. Aging (Albany. NY) *3*, 1192-1201.

Rodwell,G.E., Sonu,R., Zahn,J.M., Lund,J., Wilhelmy,J., Wang,L., Xiao,W., Mindrinos,M., Crane,E., Segal,E., Myers,B.D., Brooks,J.D., Davis,R.W., Higgins,J., Owen,A.B., and Kim,S.K. (2004). A transcriptional profile of aging in the human kidney. PLoS. Biol. *2*, e427.

Roth,S.M., Ferrell,R.E., Peters,D.G., Metter,E.J., Hurley,B.F., and Rogers,M.A. (2002). Influence of age, sex, and strength training on human muscle gene expression determined by microarray. Physiol Genomics *10*, 181-190.

Sahin,E. and Depinho,R.A. (2010). Linking functional decline of telomeres, mitochondria and stem cells during ageing. Nature *464*, 520-528.

Sherman,M.Y. and Goldberg,A.L. (2001). Cellular defenses against unfolded proteins: a cell biologist thinks about neurodegenerative diseases. Neuron *29*, 15-32.

Smyth,G.K. (2004). Linear models and empirical bayes methods for assessing differential expression in microarray experiments. Stat. Appl. Genet. Mol. Biol. *3*, Article3.

Spector,D.L. and Gasser,S.M. (2003). A molecular dissection of nuclear function. Conference on the dynamic nucleus: questions and implications. EMBO Rep. *4*, 18-23.

Srivastava,A., Wang,J., Zhou,H., Melvin,J.E., and Wong,D.T. (2008). Age and gender related differences in human parotid gland gene expression. Arch. Oral Biol. *53*, 1058-1070.

Tavanez,J.P., Calado,P., Braga,J., Lafarga,M., and Carmo-Fonseca,M. (2005). In vivo aggregation properties of the nuclear poly(A)-binding protein PABPN1. RNA. *11*, 752-762.

Taylor,E.W. (1915). Progressive vagus-glossopharyngeal paralysis with ptosis: contribution the group of family diseases. J Nerv Ment Dis *42*, 129-139.

Tome,F.M. and Fardeau,M. (1980). Nuclear inclusions in oculopharyngeal dystrophy. Acta Neuropathol. *49*, 85-87.

Trollet,C., Anvar,S.Y., Venema,A., Hargreaves,I.P., Foster,K., Vignaud,A., Ferry,A., Negroni,E., Hourde,C., Baraibar,M.A., 't Hoen,P.A., Davies,J.E., Rubinsztein,D.C., Heales,S.J., Mouly,V., van der Maarel,S.M., Butler-Browne,G., Raz,V., and Dickson,G. (2010). Molecular and phenotypic characterization of a mouse model of oculopharyngeal muscular dystrophy reveals severe muscular atrophy restricted to fast glycolytic fibres. Hum. Mol. Genet. *19*, 2191-2207.

van der Sluijs,B.M., van Engelen,B.G., and Hoefsloot,L.H. (2003). Oculopharyngeal muscular dystrophy (OPMD) due to a small duplication in the PABPN1 gene. Hum. Mutat. *21*, 553.

Verheesen,P., de Kluijver,A., van Koningsbruggen,S., de Brij,M., de Haard,H.J., van Ommen,G.J., van der Maarel,S.M., and Verrips,C.T. (2006). Prevention of oculopharyngeal muscular dystrophy-associated aggregation of nuclear polyA-binding protein with a single-domain intracellular antibody. Hum. Mol. Genet *15*, 105-111.

Welle,S., Brooks,A.I., Delehanty,J.M., Needler,N., Bhatt,K., Shah,B., and Thornton,C.A. (2004). Skeletal muscle gene expression profiles in 20-29 year old and 65-71 year old women. Exp. Gerontol. *39*, 369-377.

Welle,S., Brooks,A.I., Delehanty,J.M., Needler,N., and Thornton,C.A. (2003). Gene expression profile of aging in human muscle. Physiol Genomics *14*, 149-159.

Zahn,J.M., Sonu,R., Vogel,H., Crane,E., Mazan-Mamczarz,K., Rabkin,R., Davis,R.W., Becker,K.G., Owen,A.B., and Kim,S.K. (2006). Transcriptional profiling of aging in human muscle reveals a common aging signature. PLoS. Genet. *2*, e115.

Zhu,C.H., Mouly,V., Cooper,R.N., Mamchaoui,K., Bigot,A., Shay,J.W., Di Santo,J.P., Butler-Browne,G.S., and Wright,W.E. (2007). Cellular senescence in human myoblasts is overcome by human telomerase reverse transcriptase and cyclin-dependent kinase 4: consequences in aging muscle and therapeutic strategies for muscular dystrophies. Aging Cell *6*, 515-523.

APPENDIX

Supplementary Table 1 – A list of muscle biopsies of OPMD patients and controls. All expPABPN1 carriers were confirmed by sequence analysis.

Controls						expPABPN1 carriers					
						Pre-symptomatic			Symptomatic		
Sex	**Age**	**Sex**	**Age**	**Sex**	**Age**	**Sex**	**Age**	**MRC**	**Sex**	**Age**	**MRC**
Female	17	Male	36	Male	55	Female	37	5	Female	49	4
Male	17	Female	36	Female	56	Female	37	5	Female	54	5
Female	19	Male	36	Female	56	Male	38	5	Female	57	4
Female	19	Female	37	Male	56	Female	39	5	Male	59	5
Male	20	Female	38	Male	58	Female	39	5	Female	60	4
Female	20	Male	39	Female	58	Female	41	5	Female	60	4.5
Male	22	Female	39	Female	60				Male	66	4.5
Male	23	Male	39	Female	60				Male	68	3.5
Female	25	Male	40	Female	60				Female	69	4.5
Female	27	Male	40	Male	60						
Male	27	Male	40	Male	61						
Female	27	Female	40	Male	66						
Male	28	Male	41	Female	67						
Male	28	Male	42	Male	67						
Male	29	Male	42	Female	67						
Male	29	Male	42	Female	67						
Female	31	Male	42	Male	68						
Female	31	Male	43	Female	70						
Male	32	Male	43	Male	70						
Female	32	Female	43	Male	73						
Female	32	Female	43	Male	77						
Female	34	Female	44	Female	85						
Female	34	Male	44	Female	87						
Male	34	Male	45	Female	89						
Female	35	Female	48								
Female	35	Male	49								
Female	35	Female	49								

MRC score is a non-linear clinical measure for muscle weakness. MRC in left and right quadriceps was determined at the same day when biopsies were sampled. Values show an average of both sides. MRC in age-matching controls and in pre-symptomatic is 5. 5=normal muscle strength; <5 indicates muscle weakness.

Supplementary Table 2 - Functional Analysis of ageing and OPMD associated transcriptional changes. Biological processes are defined and clustered according to KEGG. Number of genes per pathway is depicted by #. P-value is indicated by P. The proportion of deregulated genes are depicted by %. Significant deregulation of KEGG pathways in OPMD animal models are indicated.

			Muscle Aging						OPMD			
			Human Welle et al. (2004)			Human			Human		M.M.	D.M.
Metabolism			#	*P*	%	#	*P*	%	*P*	%		
Carbohydrate	620	Pyruvate metabolism	41	1.1E-07	36.59	40	1.2E-04	37.50	-		*	*
	51	Fructose and mannose metabolism	35	3.0E-03	20.00	35	2.1E-04	48.57	2.3E-02	28.57	*	*
	562	Inositol phosphate metabolism	49	3.1E-02	16.33	47	8.2E-04	31.91	3.0E-03	17.02	*	*
Energy	190	Oxidative phosphorylation	112	1.9E-05	54.46	108	7.9E-03	28.70	1.4E-02	17.59	*	*
	910	Nitrogen metabolism	24	6.8E-05	25.00	24	2.8E-02	50.00	1.1E-02	20.83	*	*
Lipid	564	Glycerophospholipid metabolism	67	3.4E-03	19.40	64	5.0E-07	48.44	1.7E-03	18.75	*	*
	1030	Glycan structures - biosynthesis 1	118	8.8E-03	23.73	106	4.3E-03	37.74	3.3E-03	14.15	*	*
	590	Arachidonic acid metabolism	54	1.3E-02	14.81	50	2.9E-04	40.00	1.5E-02	18.00	*	
Nucleotide	230	Purine metabolism	145	5.1E-04	23.45	139	5.6E-05	43.88	5.5E-03	28.78	*	*
	240	Pyrimidine metabolism	89	1.6E-03	20.22	86	1.1E-03	36.05	1.9E-02	22.09	*	*
Amino Acid	260	Glycine, serine and threonine metabolism	42	3.6E-06	23.81	39	1.3E-03	30.77	4.4E-02	20.51	*	*
	251	Glutamate metabolism	24	1.1E-04	29.17	23	4.1E-03	47.83	4.2E-02	17.39	*	*
	271	Methionine metabolism	21	1.4E-02	28.57	20	1.2E-02	40.00	4.3E-02	25.00	*	
Glycan Biosynthesis	1032	Glycan structures - degradation	31	2.5E-02	22.58	29	1.7E-02	37.93	3.0E-03	24.14	*	
Cofactors and Vitamins	760	Nicotinate and nicotinamide metabolism	23	1.7E-06	34.78	23	2.2E-04	56.52	6.2E-03	34.78	*	*
Genetic Information Processing												
Transcription	3020	RNA polymerase	25	9.3E-04	28.00	22	3.9E-04	36.36	2.1E-02	27.27	*	*
Translation	970	Aminoacyl-tRNA biosynthesis	41	1.2E-03	24.39		-		1.2E-02	28.95	*	*
	3010	Ribosome		-		83	5.9E-03	37.35	-		*	*

			#	*P*	%	#	*P*	%	*P*	%	M.M.	D.M.
Folding, Sorting and Degradation	3050	Proteasome	43	4.7E-04	32.56		-		9.3E-03	34.09	*	*
	4120	Ubiquitin mediated proteolysis	131	1.6E-03	27.48	126	5.4E-06	45.24	1.5E-03	30.16	*	*
	4130	SNARE interactions in vesicular transport	37	1.9E-03	27.03	38	5.8E-03	34.21	3.5E-02	26.32	*	*
Replication and Repair	3030	DNA replication	36	1.4E-03	33.33	34	1.3E-03	41.18	1.5E-02	23.53	*	*
	3420	Nucleotide excision repair	43	2.9E-02	18.60	41	1.6E-03	36.59	8.9E-04	24.39	*	*

Environmental Information Processing

Membrane Transport	2010	ABC transporters - General	41	8.9E-03	24.39	44	2.1E-04	43.18	4.1E-03	25.00	*	*
Signal Transduction	4330	Notch signaling pathway	46	1.1E-05	41.30		-		2.8E-03	18.60	*	*
	4150	mTOR signaling pathway	50	2.4E-05	42.00	49	1.9E-03	44.90	1.7E-02	28.57	*	*
	4370	VEGF signaling pathway	73	1.7E-03	23.29	67	2.5E-06	43.28	5.5E-03	20.90	*	*
	4010	MAPK signaling pathway	265	1.9E-03	24.91	253	7.5E-05	39.13	5.5E-03	18.18	*	N/A
	4012	ErbB signaling pathway	87	2.0E-03	27.59	83	3.1E-06	33.73	2.3E-02	27.71	*	*
	4310	Wnt signaling pathway	148	4.4E-03	25.68	147	1.5E-04	39.46	7.6E-04	21.09	*	*
	4350	TGF-beta signaling pathway	83	7.5E-03	25.30	82	8.2E-05	39.02	9.5E-03	26.83	*	*
	4340	Hedgehog signaling pathway	53	2.0E-02	16.98	56	3.3E-02	26.79	3.7E-03	16.07	*	*
	4070	Phosphatidylinositol signaling system	76	2.2E-02	18.42	75	4.3E-03	34.67	3.4E-03	20.00	*	*
	4630	Jak-STAT signaling pathway	150	2.2E-02	19.33	145	3.9E-05	39.31	5.6E-03	19.31	*	*
	4020	Calcium signaling pathway	176	4.3E-02	21.59	169	3.1E-04	41.42	1.4E-03	18.34	*	*
Signaling Molecules	4512	ECM-receptor interaction	84	3.9E-02	20.24	79	5.3E-03	43.04	5.0E-04	27.85	*	N/A

Cellular Processes

Transport / Catabolism	4140	Regulation of autophagy	34	1.3E-03	26.47	32	2.0E-02	31.25	3.6E-02	18.75	*	*
Cell Motility	4810	Regulation of actin cytoskeleton	210	7.6E-03	22.38	204	9.8E-03	33.33	2.4E-02	16.67	*	N/A

Cell Growth and Death	4110	Cell cycle	111	1.4E-04	28.83	109	5.0E-06	42.20	6.0E-03	21.10	*	
	4115	p53 signaling pathway	68	1.4E-03	27.94	63	1.1E-06	34.92	-		*	*
	4210	Apoptosis	88	4.6E-03	23.86	78	5.4E-06	42.31	1.1E-02	21.79	*	*
Cell Communication	4510	Focal adhesion	199	9.0E-04	26.13	190	3.1E-04	44.21	3.4E-03	24.74	*	N/A
	4520	Adherens junction	74	9.5E-04	28.38	75	1.6E-02	34.67	3.8E-03	25.33	*	N/A
	4530	Tight junction	129	1.7E-03	22.48	127	1.8E-03	40.16	2.1E-02	21.26	*	N/A
	4540	Gap junction	94	8.1E-03	23.40	92	1.6E-03	40.22	9.8E-04	31.52	*	N/A
Organismal Systems												
Immune System	4660	T cell receptor signaling pathway	94	5.7E-03	23.40	86	7.0E-03	45.35	3.5E-02	15.12	*	N/A
	4670	Leukocyte transendothelial migration	113	1.3E-02	17.70	107	6.7E-03	45.79	-		*	N/A
	4664	Fc epsilon RI signaling pathway	76	1.9E-02	17.11	73	4.1E-04	45.21	1.4E-03	17.81	*	N/A
	4650	Natural killer cell mediated cytotoxicity	130	2.4E-02	17.69	121	1.5E-03	42.15	3.2E-02	11.57	*	N/A
	4620	Toll-like receptor signaling pathway	101	3.7E-02	17.82	93	1.2E-02	45.16	1.6E-02	19.35	*	N/A
Endocrine System	4910	Insulin signaling pathway	136	8.4E-04	30.88	135	3.3E-05	39.26	1.6E-03	29.63	*	N/A
	4912	GnRH signaling pathway	98	1.1E-02	23.47	95	5.0E-05	40.00	7.4E-04	30.53	*	N/A
	4916	Melanogenesis	99	1.7E-02	20.20	101	5.5E-03	30.69	6.9E-04	25.74	*	N/A
Nervous System	4720	Long-term potentiation	70	9.7E-03	25.71	68	5.9E-03	36.76	2.6E-03	25.00	*	N/A
Human Diseases												
Immune System	5340	Primary immunodeficiency	34	1.2E-02	14.71		-		3.5E-02	12.50	*	N/A
Neurodegenerative	5010	Alzheimer's disease	158	5.0E-06	46.84	151	6.5E-05	29.80	2.6E-03	21.85	*	N/A
	5012	Parkinson's disease	113	1.4E-05	58.41	104	2.3E-03	27.88	2.1E-02	18.27	*	N/A
	5040	Huntington's disease	31	2.9E-03	32.26	28	9.6E-03	42.86	5.0E-03	35.71	*	N/A
	5014	Amyotrophic lateral sclerosis (ALS)	55	6.4E-03	27.27	51	7.5E-05	37.25	1.0E-02	23.53	*	N/A

			#	*P*	%	#	*P*	%	*P*	%	M.M.	D.M.
Metabolic	4930	Type II diabetes mellitus	42	2.5E-03	35.71	41	7.4E-05	36.59	2.6E-02	19.51	*	N/A
Infectious	5130	Pathogenic Escherichia coli infection	49	1.3E-03	38.78	48	4.8E-02	45.83	2.3E-02	22.92	*	N/A
	5110	Vibrio cholerae infection	56	2.4E-03	25.00	57	5.1E-03	45.61	3.7E-03	28.07	*	N/A
	5120	Epithelial cell signaling in Helicobacter …	65	1.2E-02	20.00	62	1.6E-05	53.23	2.5E-02	29.03	*	N/A
Cancer	5211	Renal cell carcinoma	69	3.7E-05	34.78	67	1.9E-05	40.30	3.1E-02	20.90	*	N/A
	5216	Thyroid cancer	29	1.7E-04	41.38	28	4.7E-04	42.86	1.2E-02	25.00	*	N/A
	5215	Prostate cancer	90	2.3E-04	26.67	84	5.9E-03	45.24	4.7E-03	29.76	*	N/A
	5218	Melanoma	71	5.3E-04	30.99		-		3.9E-02	19.12	*	N/A
	5214	Glioma	64	7.9E-04	32.81	62	1.2E-02	38.71	5.4E-03	24.19	*	N/A
	5220	Chronic myeloid leukemia	74	8.5E-04	36.49	70	3.4E-05	32.86	2.8E-02	22.86	*	N/A
	5223	Non-small cell lung cancer	54	1.2E-03	29.63	51	1.4E-02	33.33	3.4E-02	17.65	*	N/A
	5210	Colorectal cancer	83	1.4E-03	31.33	81	2.7E-03	38.27	1.7E-02	20.99	*	N/A
	5222	Small cell lung cancer	86	2.2E-03	27.91	78	2.7E-04	53.85	1.3E-02	25.64	*	N/A
	5213	Endometrial cancer	52	2.4E-03	26.92	50	2.3E-03	40.00	3.8E-02	24.00	*	N/A
	5221	Acute myeloid leukemia	57	4.5E-03	29.82	53	1.8E-05	47.17	3.0E-02	28.30	*	N/A
	5217	Basal cell carcinoma	53	2.7E-02	18.87	53	4.3E-03	33.96	2.3E-04	16.98	*	N/A

Supplementary Table 3 – A primer list for RT-qPCR.

Gene	FW Primer	RV Primer
GUSB	5' CTCATTTGGAATTTTGCCGATT	5' CCGAGTGAAGATCCCCTTTTTA
GapDH	5' CAACGAATTTGGCTACAGCA	5' AGGGGTCTACATGGCAACTG
PABPN1	5' ATGCCCGTTCCATCTATGTTG	5' GCCTGGTCTGTTGGTTCGTT
MYH1	5' TGGACAAACTGCAAGCAAAG	5' GACCTGGGACTCAGCAATGT
CAV3	5' CTGTTGCCTGAGCACAAAAA	5' GTTAGCCAAAGGGGAGGTTC
DMD	5' TGAGAGCTTTATTGCTGCATTTT	5' CATGCCATGTGATGTTTATGC